ELSEVIER

Composite Structures 53 (2001) 333–344

COMPOSITE STRUCTURES

www.elsevier.com/locate/compstruct

Crack branching in cross-ply composites: an experimental study

Valeria La Saponara *, George A. Kardomateas

School of Aerospace Engineering, Georgia Institute of Technology, Atlanta GA 30332-0150, USA

Abstract

The objective of this research is to discuss experimental data regarding a type of failure called crack branching. The specimens tested are layered glass/epoxy and graphite/epoxy cross-ply composites, manufactured with an initial interlayer crack. Experiments were carried out under static conditions. A designed two-level two-variable experiment based on an 8×8 Hadamard matrix was performed in order to identify the key parameters of the phenomenon. Moreover, a smoothing technique (smoothing by running median of 3 repeated) was used to interpret the crack growth rate in terms of branching angles. The results indicate that there is a critical branching angle (39–40°). When the crack branches with an angle greater than this critical value, the crack growth rate increases with the branching angle. Moreover, the branching angle increases when the initial delamination decreases, for branching angles greater than the critical value. The position through the thickness does not seem to significantly affect the branching angle.

Keywords: Glass/epoxy; Graphite/epoxy; Delamination; Branching; Kinking; Cross-ply; Mixed mode bending; Double cantilever beam; Smoothing; Design

1. Introduction

Crack branching (also called crack kinking) is a type of failure that occurs in different types of structures (composites, metals, concrete, sandwich). The paper focuses on crack branching out of an interface between two layers of a composite laminate. The laminates tested are made of glass/epoxy and graphite/epoxy. They are cross-ply specimens, where 0° and 90° layers alternate. The delamination starter was inserted during the manufacture of the specimens, and consisted of a Teflon thin film between a 0° and a 90° layer. Under loading, the crack extended and branched into a different interface. This behavior repeated itself along the length of the laminate.

Branching is a phenomenon that has been discussed for about 20 years, and most work published on it has been of analytical and numerical nature, with little or no correlation with experiments. Moreover, most of these studies are based on the assumptions of either infinitesimally small kinks or infinitesimally small kink angles, for both isotropic and anisotropic materials [1–9]. Such hypotheses considerably simplify the governing equations, but may not be consistent with the experimentally determined behavior observed by the present authors: cracks branching with angles up to 90° were observed, and they crossed a distance that was of the order of 1 ply thickness.

Two types of static experiments are described here: mixed mode bending (MMB) and double cantilever beam (DCB) tests. Crack branching occurred in each of the specimens. Also La Saponara and Kardomateas [10] presented a statistical analysis of the results of fatigue tests on graphite/epoxy cross-ply specimens. The analysis shows that crack branching seems to significantly accelerate crack growth for branching angles greater than 33°. This non-intuitive result needs further investigation, as the literature provides examples of slower crack growth [11] and faster crack growth [12] under mixed mode conditions. This aspect will also be investigated in the paper.

In particular, the DCB test was designed, based on the so-called 8×8 Hadamard matrix. The objective of the test was to find the relation between the branching angle (the key variable of the problem) and two geometric features of the delamination: its initial length, and its position in the laminate. Also the variation of crack growth with the length and the position of the delamination was analyzed.

Eight specimens with specific characteristics were tested. Data could be collected from only seven out of

* Corresponding author.
E-mail address: valeria@cad.gatech.edu (V. La Saponara).

0263-8223/01/$ - see front matter
PII: S0263-8223(01)00017-4

the eight specimens, due to an unexpected failure. Since the method has been shown to be robust with respect to an outlier data, projected values for the missing test were derived from the trend of existing data, and were then used in the analysis. A complete description of the method will follow. Moreover, a smoothing technique (smoothing by running median of 3 repeated) has been used to understand the general trend of crack growth with the magnitude of the branching angle.

The results indicate that there is a critical branching angle: when a crack has a branching angle greater than this value, the branching angle increases as the initial delamination length decreases. Furthermore, the crack growth rate increases for branching angles greater than the critical value. For branching angles smaller than the critical value, the crack growth rate is for all practical purposes constant.

2. Experimental background

Previous experimental work provided some investigations for the crack branching phenomenon of specimens under static and fatigue loading. Pelegri and Kardomateas [13] considered compressive monotonic, compressive fatigue and DCB tests. They observed that the branching angle seems to increase as the delamination is located closer to the mid-plane.

Chai [14] conducted experiments on different lay-ups and interfaces with DCB tests. In his tests, branching (also called intra-ply failure) preceded and followed the interlaminar failure. According to Chai, matrix failure and 0° fibers breaking may cause branching, however the interpretation is complicated by the extensive damage at the crack tip, which could depend on the test geometry. He noticed a geometric relation between some of the features of crack branching, namely, the distance crossed in the ply thickness direction, and the distance crossed along the ply.

3. Considerations on the tests used

A crack that branches is subject to both Mode I (opening) and Mode II (shear) loading, as the crack is no longer perpendicular to the loading direction as in the classic Griffith crack model. Therefore, mixed mode tests were used to study this phenomenon: in particular, MMB and DCB tests. These latter tests are traditionally used to calculate fracture toughness and are considered typically Mode I tests. However, in a cross-ply lay-up, most times the crack branches either just before crack growth or soon after, and therefore mixed mode conditions occur. The measurement of fracture toughness in a cross-ply laminate is no trivial task as it is difficult to obtain self-similar crack growth. DCB tests were included in the study as a mixed mode test.

4. Description of the equipment

The equipment used consists of an Instron 8501 dynamic testing machine, a Questar QM-1 remote video measurement system and an Olympus BH2-UMA microscope.

The Instron 8501 is a hydraulic machine that has a load capacity of 100 kN. The QM-1 microscope is a long distance catadioptric-type Masuktov–Cassegrain, with a working range of 0.55–1.7 m and a resolution of 2.5 μm. The system includes a video-camera, a video-enhancing unit and a travel encoder digital read-out unit: this allows tri-axial motion of the microscope and a simultaneous digital measurement of distances between two arbitrary points observed by the microscope. The tests have been video-recorded and the images have been analyzed on a Silicon Graphics O2 computer. The QM-1 microscope was used during the tests to follow and measure crack growth. The specimens were coated with white paint in order to visualize the crack. The paint, however, did not allow observation of different plies in the specimens, nor the local details. The specimens were cleaned and polished after the tests, and studied with the Olympus BH2-UMA. This microscope is connected with a CCD camera. The images from the camera were sent to a monitor and then printed and scanned.

A MMB fixture, described by Reeder and Crews [15] and Reeder [16], has been used for the corresponding test. A sketch of the fixture is shown in Fig. 1.

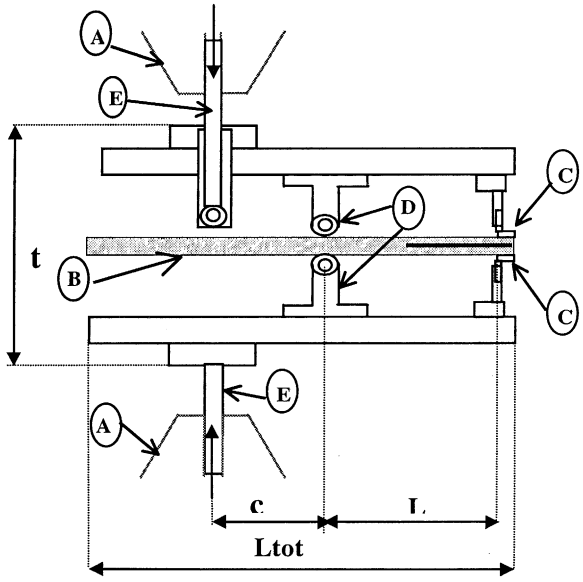

Fig. 1. MMB fixture. Ltot = 254 mm; c = 39.7 mm; L = 101.6 mm; t = 152.4 mm. Not to scale. Legend: A = Instron grip; B = specimen; C = piano hinge; D = fulcrum; E = yoke.

In the DCB test, the piano hinges attached to the specimen were directly clamped in the Instron grips.

5. Description of materials and specimens

The materials utilized are:

(a) S2/ SP250 glass/epoxy, donated by NASA Langley. Its properties are: Young's modulus in the fiber direction, $E_{11} = 45.50$ GPa; Young's modulus in the direction perpendicular to the fiber, $E_{22} = 14.50$ GPa; main Poisson's ratio, $\nu_{12} = 0.26$; shear modulus $G_{12} = 4.13$ GPa.

(b) TOHO UT500 graphite/epoxy. Its properties are: Young's modulus in the fiber direction, $E_{11} = 124$ GPa; Young's modulus in the direction perpendicular to the fiber, $E_{22} = 9.60$ GPa; main Poisson's ratio, $\nu_{12} = 0.344$; shear modulus $G_{12} = 5.75$ GPa.

The materials were in pre-impregnated (pre-preg) form. Two types of lay-ups have been prepared: 90° layers and cross-ply. The use of unidirectional 90° composites was considered for test benchmark. In fact, plenty of data are available in the literature for unidirectional 0° specimens, where branching does not occur; on the other hand, in the 90° specimens branching occurs, with the crack running through the specimen's thickness and breaking the specimen.

Table 1 shows the types of specimens used for each test, the geometry and the dimensions. The position of the delamination is expressed as the ratio of the layers in the delaminated plate, h, and the total number of layers, T.

The delamination starter consisted of an unetched Teflon film inserted in the specimen during the lay-up. The Teflon film was located at one edge of each specimen.

6. Results of the mixed mode bending tests

The MMB tests have been performed under displacement control conditions, with a rate of 2.54×10^{-3} mm/s. The Mode I and Mode II components of the applied load P, P_{I} and P_{II}, depend on the lengths c and L in the MMB fixture (Fig. 1, Eq. (1)) as given by Reeder and Crews [15] and Reeder [16]. Under the simplification of negligible weight of the fixture, the ratio of the strain energies of Mode I and Mode II, i.e., $G_{\mathrm{I}}/G_{\mathrm{II}}$, is also given in [15,16]:

$$P_{\mathrm{I}} = \left(\frac{3c-L}{4L}\right)P, \qquad P_{\mathrm{II}} = \left(\frac{c+L}{L}\right)P,$$
$$G_{\mathrm{I}}/G_{\mathrm{II}} = \frac{4}{3}\left[\frac{3c-L}{c+L}\right]^2, \quad c \geqslant \frac{L}{3}. \tag{1}$$

Therefore, by changing the ratio c/L, it is possible to have predominance of Mode I or Mode II.

The work of Reeder and Crews is applied to unidirectional specimens as self-similarity of the crack growth is sought. Eq. (1) does not apply to cross-ply specimens. Therefore, exact values of mode mixity for the tests described in this paper are not currently available, and will be the object of the future work. Approximate values may be obtained based on the unidirectional specimens by using Eq. (1).

The terminology used to describe the results is given here. The term 'primary delamination' indicates the original crack created by the delamination starter, parallel to the length of the specimen. An 'intra-layer crack' is equivalent to a 'branching crack', because it runs into the thickness of the specimen. Finally, 'secondary delamination' indicates a crack parallel to the primary delamination that is obtained once the branched crack turns in the direction parallel to the primary delamination in the same layer or at an adjacent layer interface. Most times, in the cross-ply plates, the pattern repeats, the secondary delamination extends and then branches again, and finally turns parallel to the original direction. The subsequent delaminations will still be called 'secondary'. The kink angle has been measured with respect to the direction of the crack prior to branching, and is positive if counterclockwise.

Results are as follows. Branching has been observed in all the performed tests. In the 90° unidirectional composites, there is little or no growth of the primary delamination, with branching through the whole thickness of the specimens and subsequent breaking of the specimen (Figs. 2 and 3): the failure is sudden and catastrophic. The branching angles range between 70° and 110°.

In the cross-ply specimens, the primary delamination, initially located between a 0° ply and a 90° ply, grows and subsequently kinks in the 90° layer. Then it turns

Table 1
Specimen information for each test[a]

Specimen designation	Test	Material type	Stacking sequence	Position of delamination, h/T	Average dimensions (mm)
(a)	MMB	S2/ SP250	$[(90)_{24}]$	12/24	$25.5 \times 254 \times 4.67$
(b)	MMB	S2/ SP250	$[(0/90)_{15}]$	15/30	$25.4 \times 254 \times 6.14$
(c)	MMB	S2/ SP250	$[(0/90)_{14}, 0]$	15/29	$25.3 \times 254 \times 5.94$
(d)	DCB	UT500/ Epoxy	$[(0/90)_{10}]$	10/20	$25.4 \times 137 \times 2.59$
(e)	DCB	UT500/ Epoxy	$[(0/90)_{10}]$	12/20	$25.4 \times 137 \times 2.60$

[a] MMB = mixed mode bending; DCB = double cantilever beam.

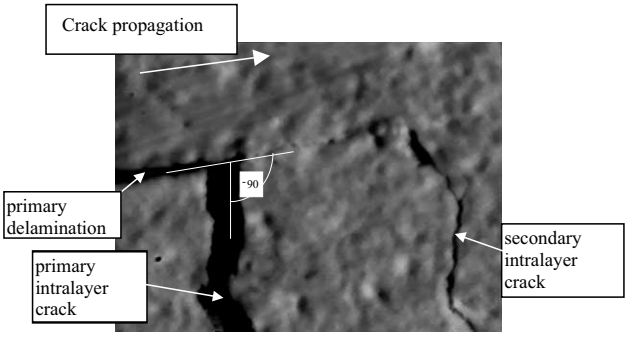

Fig. 2. Crack branching in 90° glass/epoxy specimen (type (a), Table 1).

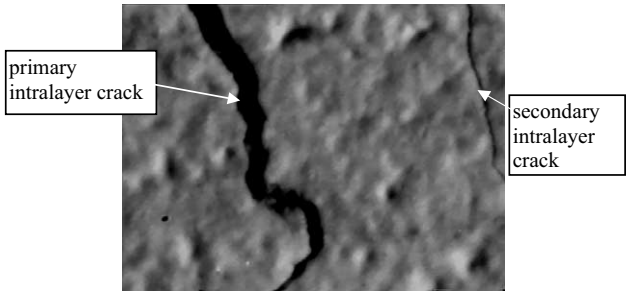

Fig. 3. Intra-layer crack in same specimen as in Fig. 2.

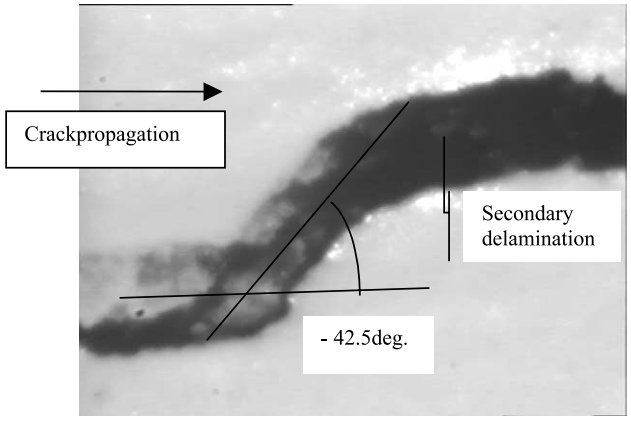

Fig. 4. Crack branching in glass/epoxy, cross-ply specimen, with initial delamination in the mid-plane (type (b), Table 1). The crack branches inside an area that is of the order of one-ply thickness (in this case 0.205 mm).

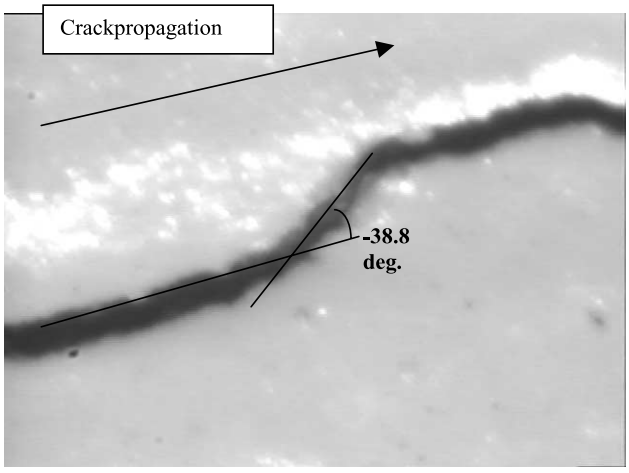

Fig. 5. Subsequent crack branching in same specimen as in Fig. 4.

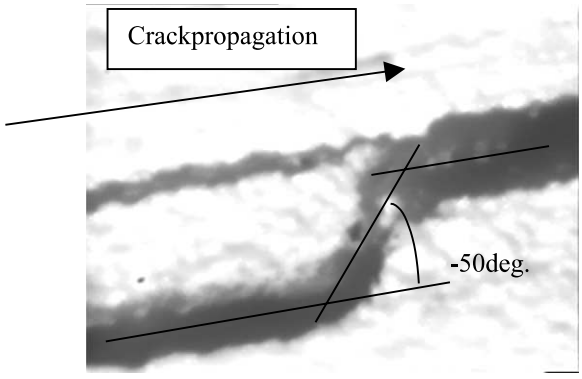

Fig. 6. Crack branching in glass/epoxy, cross-ply specimen, initial delamination one ply away from mid-plane (type (c), Table 1). The crack branches inside an area that is of the order of one-ply thickness (in this case 0.205 mm).

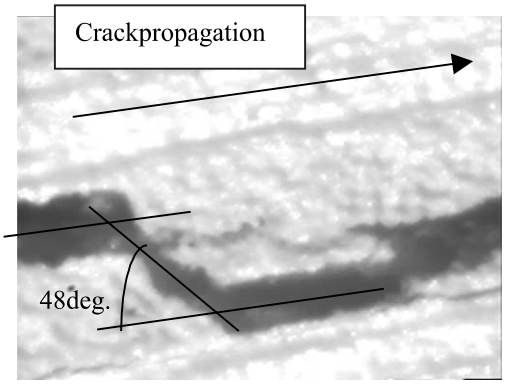

Fig. 7. Subsequent branching in same specimen as in Fig. 6.

parallel to the original direction within the same layer or at the interface with the adjacent 0° layer, and grows as secondary delamination. Afterward, it bifurcates and/or kinks again. There is no sudden and catastrophic failure as in the case of the 90° specimens. Figs. 4–7 have been taken after the MMB tests, on specimens that are still white-painted. Branching generally occurred inside one ply, that has average thickness of 0.205 mm.

The branching angles for the cross-ply specimens ranged between 29° and 55°. These angles are by no means infinitesimally small.

Fig. 8 shows the crack extension (normalized with respect to the original crack length $a0$) of four glass/

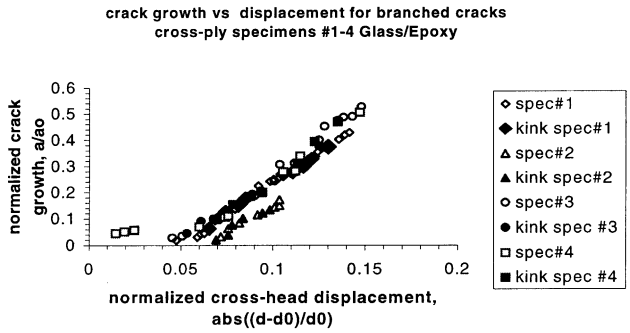

Fig. 8. Trend of normalized crack growth and branching (kink) with the normalized change of cross-head displacement of the Instron machine. $d0$ is the initial cross-head displacement. The crack growth is projected along the direction of the initial delamination, and normalized with respect to the initial delamination length, $a0$.

epoxy cross-ply specimens: specimens #1 and #2 have initial delamination in the mid-plane (type (b), Table 1), whereas specimens #3 and #4 have delamination one ply away from the mid-plane (type (c), Table 1). In all the tests, the crack growth is the projected distance along the direction of the initial delamination $a0$, and is measured starting from the end of the initial delamination. On the x-axis, the normalized change of the cross-head displacement of the Instron is given. The dark-filled symbols in the plot represent branching occurring in the specimens. It can be noticed that there is a little scatter in branching for the four specimens, no matter the position of the initial delamination. However, tests with graphite/epoxy showed less scatter, and this latter material was preferred for subsequent tests.

7. Double cantilever beam tests

The tests were performed in displacement control with a rate of 8.47×10^{-3} mm/s. Figs. 9–11 show crack growth and branching in specimens #5 and #8, and have been taken with the Olympus microscope after the test. Ply identification is possible. The initial delamination was located between a 0° and a 90° ply, but the crack started branching immediately.

Figs. 12–15 show load/displacement curves for couples of specimens with the same characteristics (namely, initial delamination length and position of the delamination). Specimen #6 is shown without the similar specimen #3 since this latter specimen failed earlier. Note that there is a high density of data points due to the sampling rate of data during the tests. The details of

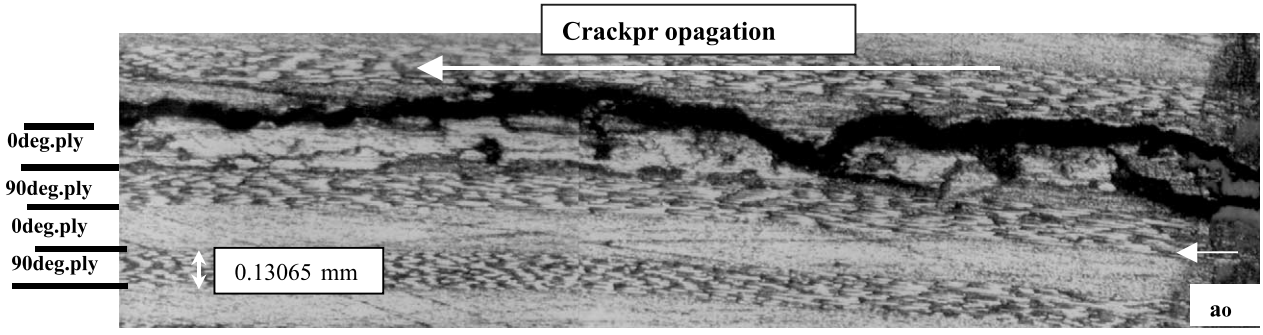

Fig. 9. Branching in DCB specimen #5 (type (d), Table 1). The end of the initial delamination is indicated with $a0$. The first 5 mm of crack growth is shown.

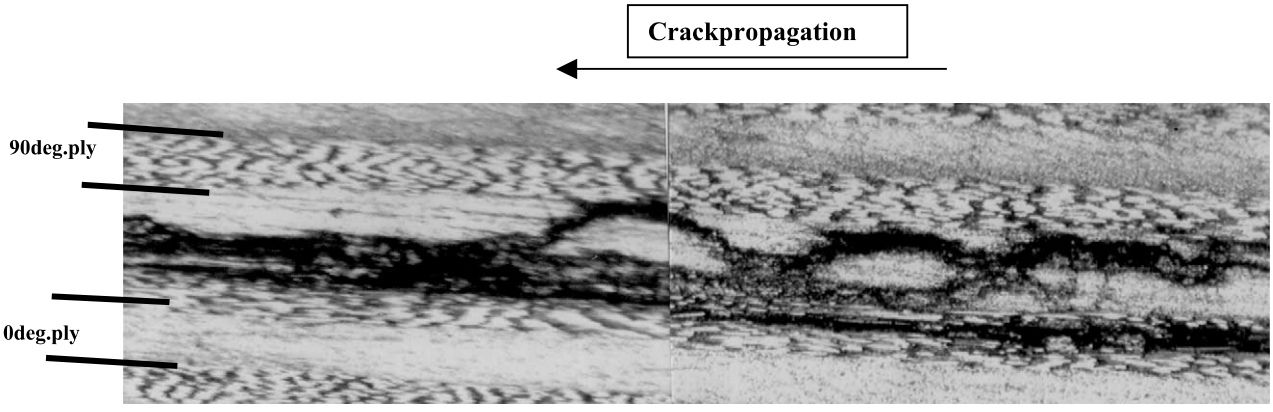

Fig. 10. Further branching in specimen #5. The picture is taken around 10 mm from the end of the initial delamination $a0$.

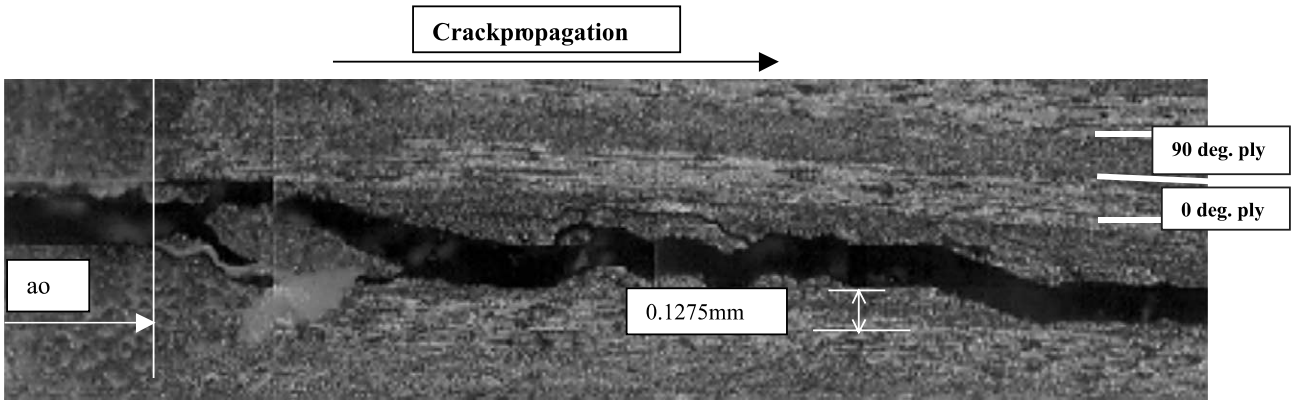

Fig. 11. Branching in specimen #8 (type (e), Table 1) from the end of the initial delamination $a0$. The first 2 mm of growth is shown.

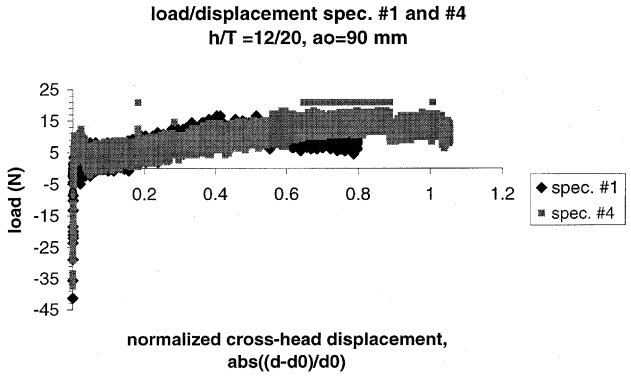

Fig. 12. Load/displacement curves for specimens #1 and #4 with same characteristics (initial delamination length $a0 = 90$ mm, and position of the delamination $h/T = 12/20$). $d0$ is the initial cross-head displacement of the Instron machine.

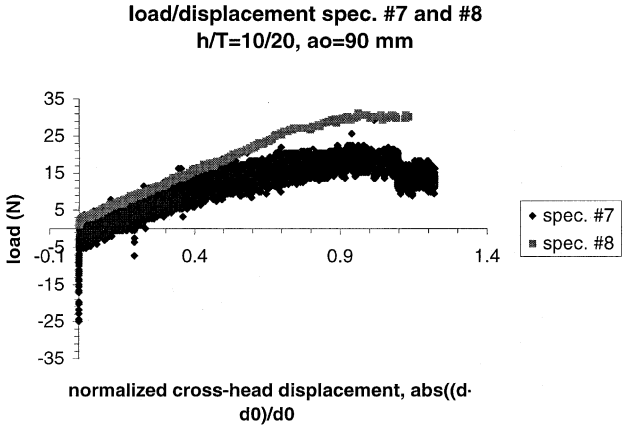

Fig. 14. Load/displacement curves for specimens #7 and #8 with same characteristics (initial delamination length $a0 = 90$ mm, and position of the delamination $h/T = 10/20$). $d0$ is the initial cross-head displacement of the Instron machine.

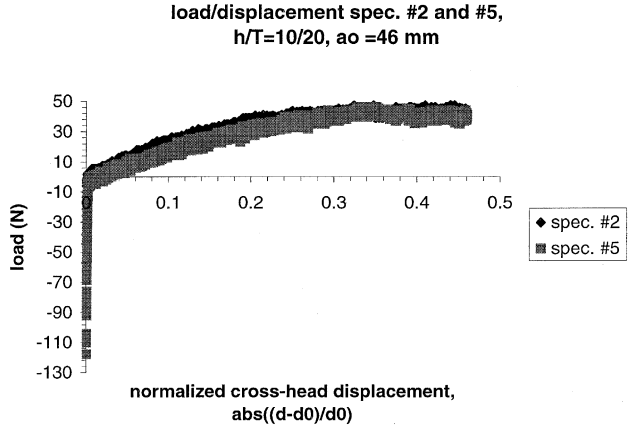

Fig. 13. Load/displacement curves for specimens #2 and #5 with same characteristics (initial delamination length $a0 = 46$ mm, and position of the delamination $h/T = 10/20$). $d0$ is the initial cross-head displacement of the Instron machine.

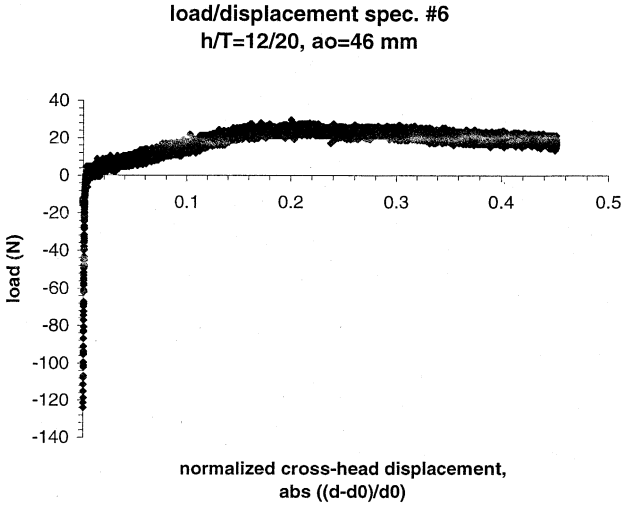

Fig. 15. Load/displacement curves for specimen #6 (initial delamination length $a0 = 46$ mm, and position of the delamination $h/T = 12/20$). $d0$ is the initial cross-head displacement of the Instron machine.

crack branching and crack growth are described in the following section.

8. Design and results of the double cantilever beam tests

The technique used for designing the DCB specimens is called 'two-level two-parameters eight-trial Hadamard matrix design': there are two parameters that change, and the analysis of the data is based on an 8×8 Hadamard matrix, composed by '+' and '−', that control how the data are summed to each other. This design allows us to derive how the two parameters, say A and B, influence the variable we are interested in (branching angle and crack growth), and how A and B interact with each other. By testing a small number of specimens (eight) designed in a specific way, it will be possible to infer these trends on a much larger number of specimens (theoretically, an infinite number), called population. The details of this design are given in [17].

By definition, a parameter assumes the 'high' level if we expect this value to be best with respect to the object of the study. The other value is assumed as 'low' level. According to the design, the treatment combination in which the parameter A has a high value is denoted as a. The treatment combination in which the parameter B has high value is denoted as b. 'ab' indicates a specimen in which both A and B have high level. The case in which both A and B have low level is indicated with '(1)' [17].

The values of A (initial delamination length) have been chosen as 46 mm (high level) and 90 mm (low level). The values of B (position of the delamination in the specimen, h/T) have been chosen as 10/20 (high level) and 12/20 (low level). The sequence of tests (also called trials) is defined in Table 2, together with the eight corresponding specimens. (*Note*: the specimens were numbered beforehand.)

The problem is as follows: we would like to know with a 90% confidence if a change of delamination length from 90 to 46 mm is going to have a significant effect on the branching angle and on the total crack growth of the population of specimens of TOHO UT500 graphite/epoxy in that configuration. Also with the same degree of confidence, we would like to know the effect of a change of delamination position from 12/20 and 10/20 on the same two variables (branching angle and total crack growth). In statistical terms, it is said that the 'alternative hypothesis' is accepted when the change is meaningful; otherwise, the 'null hypothesis' is accepted.

Table 2
Definition of the characteristics of the trials and specimens

Trial	Treatment combination	Corresponding specimen
1	a (46 mm, 12/20)	#6
2	ab (46 mm, 10/20)	#5
3	ab (46 mm, 10/20)	#2
4	b (90 mm, 10/20)	#8
5	a (46 mm, 12/20)	#3
6	b (90 mm, 10/20)	#7
7	(1) (90 mm, 12/20)	#4
8	(1) (90 mm, 12/20)	#1

After the eight specimens are tested in the sequence given in Table 2, the data of the trials (i.e., the tests) are collected and summed as in Eqs. (2.a)–(2.c) [17]:

$$\mathrm{DX}_A = (\text{trial } 1 + \text{trial } 2 + \text{trial } 3 - \text{trial } 4 + \text{trial } 5 - \text{trial } 6 - \text{trial } 7 - \text{trial } 8)/4, \quad (2.a)$$

$$\mathrm{DX}_B = (-\text{trial } 1 + \text{trial } 2 + \text{trial } 3 + \text{trial } 4 - \text{trial } 5 + \text{trial } 6 - \text{trial } 7 - \text{trial } 8)/4, \quad (2.b)$$

$$\mathrm{DX}_{AB} = (\text{trial } 1 - \text{trial } 2 - \text{trial } 3 + \text{trial } 4 + \text{trial } 5 + \text{trial } 6 - \text{trial } 7 - \text{trial } 8)/4, \quad (2.c)$$

where DX_A, DX_B and DX_{AB} are, respectively, the changes in the parameters A, B and AB (this latter indicating the interaction). These changes are then compared with a critical change used as the choice criterion, and hence the decision is made. The criterion is calculated after having derived an estimate of the variance from four columns of the 8×8 Hadamard matrix, and a Student t distribution is used to take into account the fact that the variance is not known a priori. In particular, four values of the variance S^2 are calculated from the third, fifth, sixth and seventh columns of the 8×8 Hadamard matrix, and then are averaged. The final value of the square root of the variance, the standard deviation S, is used for the test criterion:

$$|\mathrm{DX}|^* = t_\alpha S \sqrt{\frac{1}{N_{\text{high}}} + \frac{1}{N_{\text{low}}}}, \quad (3)$$

where t_α is the value of the Student t distribution corresponding to the degrees of freedom of the problem (four, in this case) and to $\alpha = 1$-level of confidence (0.10 in this case). N_{high} and N_{low} are the number of specimens having a given value (defined as high or low) of the parameters A and B. These two numbers are supposed to be always equal to each other. In this case, they should be both four. Finally, the test criterion is the following: if $|\mathrm{DX}_A| > |\mathrm{DX}|^*$ (A is used as an example), then the alternative hypothesis is accepted, i.e., a significant increase in the study variable happens when the value of A changes. This can be accepted for the population of specimens with 90% confidence.

Table 3 shows the results obtained for each specimen. Both sides of the specimen were observed. In specimen #3, the bond between the piano hinge and the specimen failed before any crack growth; therefore no data are reported. The branching angles are considered positive when counterclockwise with respect to the direction of the crack prior to branching. The angles are reported in

Table 3
Data of branching angles and crack growth for each side of the designed specimens[a]

Specimen	Branching angles		Total crack growth	
	Side 1 (deg.)	Side 2 (deg.)	Side 1 (mm)	Side 2 (mm)
#1	16, 50	Same (opposite sign)	27	26
#2	−36, 25, −46.5, 46.5, −71, 47, −49, 50, −47, 11	29, 20.5, −47, −37, 56, 22	20	20
#3	Earlier bond failure	Earlier bond failure	Earlier bond failure	Earlier bond failure
#4	−38, 39, 14.5, 41	−40, −31.5, 38, −78	27	20
#5	25, 36.5, −66.5, 24.5, −61.5, 41.5, −42, 36.5, −55.5, 36, −41	Same (opposite sign)	16	16
#6	−14, 49, 38.5, −62	Same (opposite sign)	16	25
#7	−26.5, 41, −31.5, 33, −51.5, 61.5, −60, 40, −47, −39, −49, 40, −40.5, 39	−28, 47, −30, 18, 37, −26, 30.5, −33, 56, −29, −22, 23, −45, −40, −60, 32, −29, −42	25.2	21
#8	−54, 24, 56, −45, 42, −18, −36, 33, −39, 48, 45.5, −40, 32.5	Same (opposite sign)	18	22.42

[a] The crack growth is calculated as projection along the direction of the initial delamination.

Table 4
Medians of branching angles (in magnitude), normalized crack growths and crack speeds[a]

Trial	Specimen	Median branching angles, deg.	Median normalized crack growths $a/a0$	Median crack speed (mm/s)
1, *a*	#6	43.75	0.446	5.69×10^{-3}
2, *ab*	#5	41	0.348	4.44×10^{-3}
3, *ab*	#2	39.875	0.435	5.55×10^{-3}
4, *b*	#8	40	0.225	1.60×10^{-3}
5, *a*	#3	Earlier bond failure	Earlier bond failure	–
6, *b*	#7	35.75	0.257	2.43×10^{-3}
7, (1)	#4	38.75	0.261	2.88×10^{-3}
8, (1)	#1	33	0.294	3.98×10^{-3}

[a] The crack growth a is measured as projection on the direction of the initial delamination $a0$. The crack speed is calculated at a 8.47×10^{-3} mm/s displacement rate.

the sequence in which they occurred during crack growth. On the other side of the specimen, the behavior was either the same or different. In the first case, the branching angles have the same magnitude but different 'sign': if a positive branching angle occurs on Side 1, a negative branching angle will be on Side 2. The total crack growth reported is the projection of the crack growth in the direction of the initial delamination.

The number and format of data do not allow an easy processing: each specimen had several branches, and generally different crack growths. To simplify the process, we decided to work with the medians of those data. If we have an ordered sample of n points, say y_i, with $y_i < y_{i+1}$, the median is the point that divides the sample into two equal halves. If n is even, the median is given by $(y_{n/2} + y_{(n/2)+1})/2$. The median is a robust choice as it is less sensitive to outliers of the sequence with respect to an average of the numbers of the sequence.

The medians of the magnitudes of the branching angles have been calculated for each side of each specimen, and then the results from the two sides have been averaged. The same has been done with the crack growths. Moreover, the crack growths have been normalized with respect to the initial delamination lengths. Also the average speed of crack growth (mm/s) has been reported, at the displacement rate used, 8.47×10^{-3} mm/s. Results are reported in Table 4 in the order requested by the design.

It can be observed that the median branching angles range from 33° to about 44°: the scatter of data in Table 4 has been noticeably reduced when calculating the medians. There is no evident pattern between branching angles and median normalized crack growth. As far as the median crack speed, the highest values correspond to specimens with a 46-mm delamination (specimens #2, #5 and #6). There is no apparent pattern of the median crack growth with respect to the position of the delamination: specimens #2 and #5 have delamination located in the mid-plane $(h/T = 10/20)$ and specimen #6 has delamination located two plies away from the mid-plane $(h/T = 12/20)$.

To proceed with the analysis, it has been decided to project data for specimen #3: the design in [17] does not anticipate a failure in the set of tests due to a different cause (in this case, the bond between piano hinge and the surface of specimen #3). A great advantage of the design chosen is that it is possible to make it robust with respect to external causes if the specimens are tested in a specific time sequence. The technique of choosing the time sequence is called 'blocking' [17] and it is applied to

this design. The purpose of blocking is to avoid that a change in external conditions (for example, something happening in the testing machine or a change in the temperature of the testing room) influences the overall changes DX_A, DX_B and DX_{AB} mentioned earlier. If the specimens are tested according to blocking principles, then the design is robust with respect to some outlier data. Blocking principles have been respected in our case. This allows us to include a projection of the results that specimen #3 might have given, and have a robust design in case this projection is an outlier.

In particular, we decided to use the data of the seven 'successful' specimens to project the behavior of the missing specimen. This type of extrapolation is common practice to interpret experimental data. Also even in case that the projected data from the missing specimen were not realistic, the design would not be greatly influenced by them due to the blocking technique used.

With reference to Table 4, the change between median branching angles for couples of specimens of the same type (*b*, *ab*, (1)) has been calculated. The maximum change is 17%, for specimens of the type (1). A change of ±20% has been calculated for the branching angle of specimen #6, corresponding to the same type of specimen #3. Thus, two predictions for the median branching angles have been obtained: 35° and 52.5°. Both are reasonable values. Afterward, the trend of the existing seven normalized crack growth values has been derived with respect to the seven existing median branching angles. A third-order polynomial has been chosen as fitting line (in a least-squares sense). The polynomial is a good fit except for two data points: (39.875, 0.435), and (40, 0.225), corresponding, respectively, to specimens #2 and #8 (different type from specimen #3's).

The equation of the fitting line is $y = -0.0002149x^3 + 0.02791x^2 - 1.172x + 16.31$, where y is the median normalized crack growth, and x is the median magnitude of the branching angle. Fig. 16 shows the data, the fitting line and the projection for specimen #3 based on the third-order polynomial.

Finally, the interval [35°, 52.5°] has been divided in to 70 parts with step 0.25°. The changes DX_A, DX_B, DX_{AB}, as well as the criterion $|DX|^*$ have been calculated for the seven specimens and for the projected values of specimen #3, with the branching angles for specimen #3 ranging between 35° and 52.5°.

Table 5 shows how the branching angles (in magnitude) and normalized crack growth are affected by

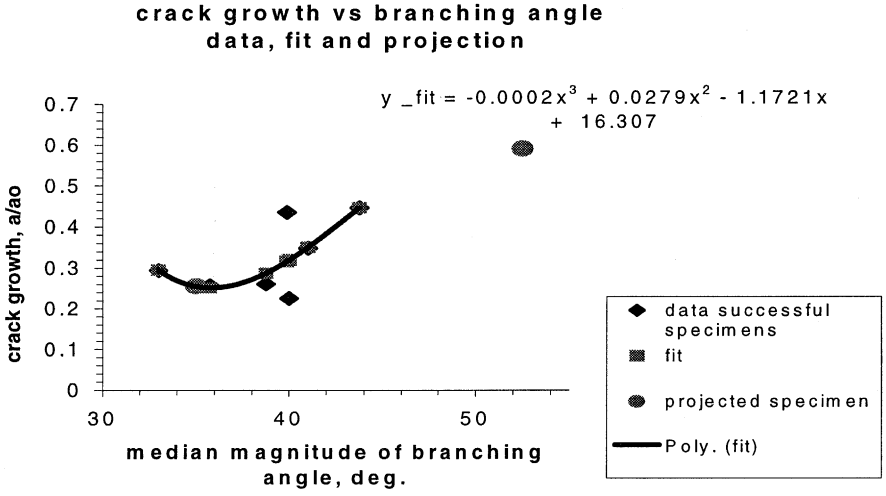

Fig. 16. Existing data for the seven successful specimens and projection of data for specimen #3, with a third-order polynomial as fit. The equation of the fit is shown.

Table 5
Effects of crack length ($a0$) change and crack length position (h/T) change[a]

	Projected branching angle range, specimen #3 (from available data and statistics), deg.	Effect of change of $a0$ from 90 to 46 mm	Effect of change of h/T from 12/20 to 10/20
Magnitude of branching angles for the population	[35–37.5]	No significant change	No significant change
	[37.75–52.5]	Significant increase	No significant change
Normalized crack growth for the population	[35–43]	Significant increase	No significant change
	[43.25–52.5]	Significant increase	Significant increase

[a] The branching angle and crack growth depended on projections for specimen #3.

Table 6
Effect of the interaction of crack length change and crack length position

	Projected branching angle range, specimen #3 (from data and statistics), deg.	Effect of interaction of change of initial crack length and position of the crack
Magnitude of branching angles for the population	[35–44]	No significant change
	[44.25–52.5]	Significant increase
Normalized crack growth for the population	[35–52.5]	No significant change

Table 7
Critical branching angle (by magnitude) calculated from the statistical analysis of experimental data, and corresponding effect[a]

Critical branching angle (deg.)	Effect
39.31	Significant increase of *branching angle* as $a0$ varies from 90 to 46 mm
39.94	Significant increase of *crack growth* as h/T changes from 12/20 to 10/20
39.94	Significant increase of *branching angle* due to the interaction of the parameters $a0$ and h/T

[a] $a0$ = initial crack length; h/T = position of delamination in the specimen (10/20 = mid-plane).

changes in the delamination length and position of the delamination. The values of the branching angles for specimen #3 influence most of the results. These findings are accepted for the population with a 90% confidence. Table 6 shows the effect of the interaction of the two parameters (initial crack length and position of initial crack length).

Finally, the critical branching angle for the set of eight specimens has been calculated corresponding to the values of the branching angle calculated for specimen #3. 'Critical' is intended as the value at which a behavior changes. For example, with reference to Table 5, 37.75° is the critical value of specimen #3 angle, as the change of initial delamination length becomes significant for median branching angles of the whole population. The critical values for specimen #3 have been selected to calculate the critical branching angle as the median angle for the set of eight specimens. The whole population is affected in varied ways, with a 90% confidence. This is shown in Table 7.

9. Discussion of the results from the designed experiment

Tables 5 and 6 show how the behavior of the population is affected from the values of the branching angles attributed to specimen #3. Also crack growth is significantly increased when the initial delamination $a0$ changes, but is not affected by specimen #3. Branching angles are not affected by a small change in the position of the delamination, and are not affected by specimen #3. In all the other cases, the behavior changes corresponding to a key value attributed to specimen #3. This key value has been used to calculate a critical value for the median branching angles (in magnitude): Table 7 shows that a value of 39–40° is critical for the behavior of the population: branching angles and crack growth increase, respectively, with a change of $a0$ and a change of h/T, the initial position of the delamination in the laminate. Also the interaction between crack growth and branching angle becomes significant at that critical value, and affects the branching angle magnitude.

However, it is not clear how branching angle and crack growth are related, since Table 6 shows that the crack growth is not significantly affected by such interaction: this seems to contradict what is shown in other parts of Table 6. A smoothing technique has been applied to the median crack growth speed and the median magnitudes of branching angles, reported in Table 4. This technique, called 'smoothing by running median of 3 repeated', was introduced by Tukey [18], and has already been used by La Saponara and Kardomateas [10]. It gives a general trend of data, not the local detail. The technique will be summarized here: the branching angles are arranged in ascending order. The corresponding crack speeds are identified. These latter values are grouped in specific sets of three, and the median of the set is taken as the smoothing value. The smoothing is repeated until the 'rough' (the difference between the data and the smooth) is minimized. Details of the technique are given in [18,10] and will not be reported here.

Fig. 17 shows the result of the smoothing on the seven specimens. The original data are reported as well. Data and smoothing were obtained from the medians of a much larger number of data.

Fig. 17 shows that there is a critical value for the median branching angle, for which the median crack speed increases. The critical value (about 40°) from the smoothing technique is consistent with the critical value from the designed experiment (39–40°). It should be repeated here that Fig. 17 was obtained using only the data of the available seven specimens. The trend of Fig. 17 seems to confirm the validity of the choices for specimen #3 in the previously mentioned design.

10. Conclusions

The paper reports the results of static experiments, namely, MMB and DCB tests, performed on glass/

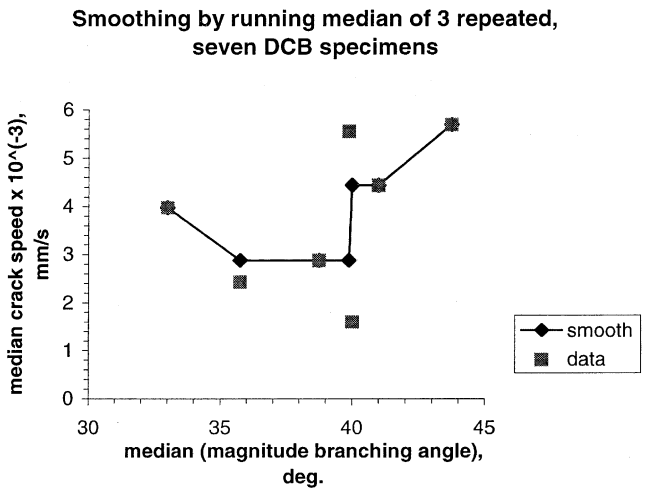

Fig. 17. 'Smoothing by running median of 3 repeated' of the median crack speeds with respect to the median branching angle (in magnitude), for the seven DCB specimens. The crack growth rate is calculated for tests with 8.47×10^{-3} mm/s displacement rate.

epoxy and graphite/epoxy cross-ply specimens. A Teflon film was inserted in the specimens as delamination starter. The crack propagated with branching and bifurcation. The DCB test has been designed, and the problems and choices of the design have been reported in detail. Also a 'smoothing by running median of 3 repeated' technique was applied to identify the general trend of median crack speeds and median branching angles for the DCB specimens. The results of the designed test and of the smoothing technique show that there is a critical branching angle at which the crack growth and the branching angles of the population of specimens are significantly affected. If a crack branches with a branching angle greater than this critical value, the branching angles increase with a decrease of initial delamination length. For branching angles smaller than this critical value, the branching angles do not seem to be affected by a change in delamination length. Most importantly, for branching angles greater than this critical value, the crack growth rate increases as the branching angles increase. For branching angles smaller than this critical value, the crack growth rate is constant.

It should be noticed that a similar result was obtained for T7G145/F1914 graphite/epoxy specimens under compressive fatigue loading, as reported in [10]: in particular, a significant increase in crack growth was noticed for branching angles greater than 33°.

The following hypothesis will be investigated upon in the future: below a critical branching angle, along the branching crack there are contact areas that lead to a delayed crack growth; for branching angles greater than the critical value, the branching crack opens and crack growth is subsequently accelerated.

This hypothesis may also justify the different findings of Suresh [11] and Iida and Kobayashi [12]. Suresh mentions 'roughness-induced closure' due to crack deflection, and therefore he experiences a slower crack growth rate. He might have found branching angles that were lower than the critical value, with closure in the branching crack. Iida and Kobayashi, on the other hand, do not mention crack closure but state that the crack deflection and the presence of a Mode II component in the loading 'increase the crack propagation rate significantly'. They might have come across branching angles greater than the critical value, with negligible crack closure.

Moreover, this behavior may not depend strongly on testing conditions and specimen geometry: in fact, the specimens tested with static DCB tests and with compressive fatigue tests [10] have very different loading conditions and geometry, but the critical branching angles seem to range between 33° and 40° in both configurations.

Acknowledgements

The financial support of the National Rotorcraft Technology Center through CERT, Grant NCC2-945, and the Office of Naval Research, Ship Structures S & T Division, Grant N00014-90-J-1995, and the interest and encouragement of the Grant Monitors, Dr. T. K. O' Brien, Dr. G. Anderson and Dr. Y. D. S. Rajapakse are both gratefully acknowledged.

The authors are also thankful to Zonta International Foundation and Clare Booth Luce Foundation.

References

[1] He M, Hutchinson JW. Kinking of a crack out of an interface. J Appl Mech 1989;56:270–8.
[2] Cotterell B, Rice JR. Slightly curved or kinked cracks. Int J Fract 1980;16(2):155–69.
[3] Obata M, Nemat-Nasser S, Goto Y. Branched cracks in anisotropic elastic solids. J Appl Mech 1989;56:858–64.
[4] Hayashi K, Nemat-Nasser S. Energy release rate and crack kinking under combined loading. J Appl Mech 1981;48:520–4.
[5] Hayashi K, Nemat-Nasser S. On branched, interface cracks. J Appl Mech 1981;48:529–33.
[6] Mukai DJ, Ballarini R, Miller GR. Analysis of branched interface cracks. J Appl Mech 1990;57:887–93.
[7] Wang TC, Shih CF, Suo Z. Crack extension and kinking in laminates and bi-crystals. Int J Solids Struct 1992;29(3):327–44.
[8] Gupta V, Argon AS, Suo Z. Crack deflection at an interface between two orthotropic media. J Appl Mech 1992;59:S79–87.
[9] Chiang CR. Kinked cracks in an anisotropic material. Eng Fract Mech 1991;39(5):927–30.
[10] La Saponara V, Kardomateas GA. Statistical considerations in the analysis of data from fatigue tests on delaminated cross-ply graphite/epoxy composites. J Eng Mater Technol 2000;122:409–14.
[11] Suresh S. Crack deflection: implications for the growth of long and short fatigue cracks. Metall Trans A 1983;14A:2375–85.
[12] Iida S, Kobayashi AS. Crack propagation rate in 7075-T6 plates under cyclic tensile and transverse shear loading. J Basic Eng 1969;91:764–9.

[13] Pelegri AP, Kardomateas GA. Intralayer cracking in delaminated glass/epoxy and graphite/epoxy laminates under cyclic or monotonic loading. In: Collection of technical papers – AIAA/ASME/ASCE/AHS/ASC structures. 1998 Apr 20–23; Long Beach, CA, USA. p. 1534–44.
[14] Chai H. The characterization of Mode I delamination failure in non-woven, multidirectional composites. Composites 1984; 15(4):277–90.
[15] Reeder JR, Crews Jr JH. Mixed mode bending method for delamination testing, AIAA J 1990;28:1270–6.
[16] Reeder JR. An evaluation of mixed-mode delamination failure criteria. NASA Technical Memorandum 104210, 1992.
[17] Diamond WJ. Practical experiment designs for engineers and scientists. New York: Wiley; 1989.
[18] Tukey JW. Exploratory data analysis. Reading, MA: Addison-Wesley; 1977.